The Meteoritical Society

Meteoritics & Planetary Science 47, Nr 5, 806–819 (2012)
doi: 10.1111/j.1945-5100.2012.01351.x

Experimental determination of photostability and fluorescence-based detection of PAHs on the Martian surface

Lewis R. DARTNELL[1,2*], Manish R. PATEL[3], Michael C. STORRIE-LOMBARDI[4], John M. WARD[5], and Jan-Peter MULLER[6]

[1]UCL Institute for Origins, University College London, UK
[2]The Centre for Planetary Sciences at UCL/Birkbeck, Earth Sciences, University College London, London, UK
[3]Department of Physical Sciences, The Open University, Milton Keynes, UK
[4]Kinohi Institute, Pasadena, California, USA
[5]Institute of Structural and Molecular Biology, University College London, UK
[6]Mullard Space Science Laboratory, Department of Space and Climate Physics, University College London, UK
[*]Corresponding author. E-mail: l.dartnell@ucl.ac.uk

(Received 05 October 2011; revision accepted 04 March 2012)

Abstract–Even in the absence of any biosphere on Mars, organic molecules, including polycyclic aromatic hydrocarbons (PAHs), are expected on its surface due to delivery by comets and meteorites of extraterrestrial organics synthesized by astrochemistry, or perhaps in situ synthesis in ancient prebiotic chemistry. Any organic compounds exposed to the unfiltered solar ultraviolet spectrum or oxidizing surface conditions would have been readily destroyed, but discoverable caches of Martian organics may remain shielded in the subsurface or within surface rocks. We have studied the stability of three representative polycyclic aromatic hydrocarbons (PAHs) in a Mars chamber, emulating the ultraviolet spectrum of unfiltered sunlight under temperature and pressure conditions of the Martian surface. Fluorescence spectroscopy is used as a sensitive indicator of remaining PAH concentration for laboratory quantification of molecular degradation rates once exposed on the Martian surface. Fluorescence-based instrumentation has also been proposed as an effective surveying method for prebiotic organics on the Martian surface. We find the representative PAHs, anthracene, pyrene, and perylene, to have persistence half-lives once exposed on the Martian surface of between 25 and 60 h of noontime summer UV irradiation, as measured by fluorescence at their peak excitation wavelength. This equates to between 4 and 9.6 sols when the diurnal cycle of UV light intensity on the Martian surface is taken into account, giving a substantial window of opportunity for detection of organic fluorescence before photodegradation. This study thus supports the use of fluorescence-based instrumentation for surveying recently exposed material (such as from cores or drill tailings) for native Martian organic molecules in rover missions.

INTRODUCTION

Organics on Mars

Mars may have provided in its early history surface environmental conditions conducive for an independent origin of life. Refuges of surficial microbial life may persist today, or at least pockets of dead microbial cells and the organic compounds produced by their degradation. Even in the absence of biology on Mars, organic molecules would be expected on the surface from delivery from space.

Many organic molecules are now known to be produced by astrochemistry in the interstellar medium and circumstellar regions (Herbst and van Dishoeck 2009), and become incorporated in the planet-forming disks of new star systems (Shaw 2007). Organic compounds are common in certain kinds of meteorites, the carbonaceous chondrites, as well as comets (Ehrenfreund and Charnley 2000), and so extraterrestrial

delivery aboard micrometeorites, meteorites, asteroids, and comets could have been a significant determinant of the organic inventory of the early Earth and Mars (Pierazzo and Chyba 1999), and continue to deliver organics to the Martian surface today. Carbonaceous chondrites are rich in a diverse repertoire of organic molecules of importance to life (Pizzarello 2006), including amino acids, carboxylic acids, aliphatic and aromatic hydrocarbons, alcohols, aldehydes, ketones, sugars (see reviews in Botta and Bada 2002; Sephton 2002; and Martins 2011), as well as purine and pyrimidine nucleobases (Martins et al. 2008). The total current annual arrival of unaltered organic material to the Martian surface (which has not been thermally degraded by atmospheric entry or impact) has been estimated to be around 2.4×10^5 kg/yr, and if this accretion rate were to have been constant over the history of the solar system, Mars would have received an amount of extrinsic carbon greater than the terrestrial biomass (Flynn 1996).

Despite this presumed long-term in-fall of diverse extrinsic organic molecules, no organics have yet been discovered. The Viking GC-MS experiments failed to detect organics in their samples of heated soil (Biemann et al. 1977). It has therefore been long believed that delivered organic material is destroyed on the Martian surface, probably by chemical reactivity of the soil itself (Quinn and Zent 1999; Benner et al. 2000; Yen et al. 2000; ten Kate 2010). Organics protected from oxidization chemistry and solar ultraviolet radiation, perhaps inside surface rocks, within permanently shadowed overhangs or caves, or deeper in the subsurface, may persist on Mars, and represent an enticing target for detection instrumentation on Martian lander and rover missions.

Fluorescence-Based Instrumentation for Detecting Martian Organics

Instruments designed to detect organics on Mars include gas chromatography mass spectrometry (GCMS), as installed aboard Mars Science Laboratory (Mahaffy 2008) and proposed for ExoMars-C (Evans-Nguyen et al. 2008; Goesmann et al. 2009); Raman spectroscopy (Ellery and Wynn-Williams 2003; Jorge Villar and Edwards 2006; Marshall et al. 2010; Rull et al. 2010), and antibody-based systems such as the Life Marker Chip (Sims et al. 2005). Such instrumentation can offer very high sensitivity and discriminatory power, but often require sample preparation, long exposure times, or limited resources or reagents. It has been proposed therefore to use an instrument based on exciting native autofluorescence from Martian organics, or perhaps even organisms, to rapidly survey potential target regions for evidence of organic content or triage samples before scrutiny with more discriminatory instruments (Aubrey et al. 2008; Griffiths et al. 2008; Storrie-Lombardi et al. 2008, 2009; Weinstein et al. 2008; Muller et al. 2009; Storrie-Lombardi and Sattler 2009; Dartnell et al. 2010, 2011). Absorption of short wavelength light by many organic molecules is often followed by relaxation of electronic excited states via emission of fluorescence. The excitation and emission spectra are characteristic of different molecules, and so fluorescence-based instrumentation can be used to both localize and identify organics. Fluorescence-based detection systems have proved themselves to be sensitive and discriminatory, and have been used in terrestrial applications for assessing pollution (JiJi et al. 1999; Ko et al. 2003; Alberts and Takács 2004; Cory and McKnight 2005), identifying potentially pathogenic or toxic microorganisms in environmental water or food preparation (Patra and Mishra 2001; Hua et al. 2007; Sohn et al. 2009; Ziegmann et al. 2010), and detecting trace biomolecules or microbial life in glacial (Rohde and Price 2007) and Antarctic ice (Storrie-Lombardi and Sattler 2009), Antarctic sandstone (Nadeau et al. 2008), and the Atacama desert (Weinstein et al. 2008).

Polycyclic Aromatic Hydrocarbons (PAHs)

One category of molecules that is of particular interest to the possibility of detecting organics on Mars is the polycyclic aromatic hydrocarbons (PAHs). PAHs are common in the interstellar medium and star-forming regions, as well as comets and carbonaceous chondrite meteorites (Herbst and van Dishoeck 2009). Botta and Bada (2002) summarize the abundance of different meteoritic organic compounds, and report concentrations of over 1000 ppm of aromatic hydrocarbons in carbonaceous chondrites. PAHs have also already been detected in Martian material; in the shergottite meteorites EETA79001 and ALH 84001 (Botta et al. 2008), rocks which formed on Mars before being ejected by an impact. PAHs are also commonly formed by biological degradation, such as found in terrestrial oil deposits, and the debate continues as to whether the PAH deposits within ALH 84001 (Clemett et al. 1998) represent decay products of Martian organisms (McKay et al. 1996; Becker et al. 1999; Gibson et al. 2001). Aliphatic hydrocarbons and PAHs may also have been synthesized in situ on Mars by Fischer-Tropsch type reactions of hydrogen- and carbon-monoxide-rich volcanic and impact gasses or hydrothermal fluids (Zolotov and Shock 1999). However, the expected PAHs, or indeed any organic molecules, have not yet been detected in situ on the Martian surface.

In addition to representing a promising molecular target from prebiotic chemistry or even microbial decay,

PAHs are highly fluorescent. PAHs exhibit such intrinsic fluorescence because the delocalized pi-orbital electrons within the aromatic rings are readily excited, and this energy is reemitted as fluorescence with a high quantum efficiency, as the rigid molecular structure does not allow for efficient vibrational relaxation. The fluorescent emission spectra can also be distinctively characteristic of particular PAHs, depending upon the number and arrangement of aromatic rings (Howerton et al. 2002). This sensitivity combined with discriminatory power has allowed the development of fluorescence-based instrumentation for applications such as detecting low levels of oil-derived PAH pollutants in seawater (Rudnick and Chen 1998) or PAH-contaminants in soil (Ko et al. 2003).

Here, we continue our recent work (Storrie-Lombardi et al. 2008; Muller et al. 2009; Storrie-Lombardi and Sattler 2009; Storrie-Lombardi et al. 2009; Dartnell et al. 2010, 2011) on the utilization of fluorescence for surveying for Martian organics or organisms, looking now specifically at the fluorescence of PAHs and the rate of degradation of this signal from unfiltered solar UV radiation. Such an instrument could employ either UV laser-induced fluorescence for remote detection, or use UV LEDs with a close-up imager (such as the Mars hand lens imager, MAHLI, aboard Mars Science Laboratory, which has two 365 nm LEDs for UV illumination at night; Edgett et al. 2009).

If a Mars exploration mission is to detect localizations of organics, they must have been protected from solar UV. Whilst protection from direct insolation is provided by shadowed overhangs, calculated by Moores et al. (2007) to offer UV flux reduction down to around 2×10^{-5} that of exposed regions, atmospheric scattering of UV radiation means that even permanently shadowed areas accumulate large doses of UV over geological periods. Detection of Martian organics can be optimized by examining previously shielded material freshly uncovered by the probe. A rock abrasion tool (RAT) such as carried by the Mars Exploration Rovers Spirit and Opportunity (Gorevan et al. 2003), the rock coring drill on Mars Science Laboratory (Okon 2010) and the 2 m subsurface drill proposed for ExoMars-C (Vago et al. 2006) are all appropriate devices for this. Once exposed to the unfiltered solar UV spectrum on the Martian surface, however, any PAHs will be readily photodegraded and their fluorescence signal lost. So the key question for the detection of PAHs and other aromatic prebiotic organic molecules is: on what time scale are they destroyed by solar UV once uncovered? What is the window of opportunity for detection by instrumentation aboard a rover?

Previous exposure experiments under Martian surface conditions have been conducted on simple organic molecules to assess ultraviolet photostability (ten Kate et al. 2005, 2006; Garry et al. 2006; Peeters et al. 2009; Stalport et al. 2009). Here, we conduct an assessment of the photostability of three PAHs, anthracene, pyrene, and perylene; representative of PAHs with three, four, and five aromatic rings, respectively (see molecular structures shown in Fig. 1). These compounds are significant both due to their expected prevalence on Mars and possibility for detection through fluorescence.

The fluorescence response from a target can be quantitatively described by the generation of an excitation-emission matrix (EEM). Briefly, an EEM is created by recording the fluorescent emission spectrum from an experimental sample across a range of excitation wavelengths, and plotting the fluorescence intensity produced at each excitation-emission wavelength combination as a contour map. Figure 1 displays EEMs of the three PAHs considered here. For further details on the production of EEMs, see the fluorescence spectroscopy methodology presented in Dartnell et al. (2010). Figure 1 shows the peak excitation wavelengths thus determined for each PAH (indicated with horizontal solid lines), as used in this study to track the UV-induced degradation of PAHs under Martian surface conditions. Dashed horizontal lines in Fig. 1 indicate other wavelengths available from commercial laser diode and LED (which can have full width at half maximum spectral spreads of around ± 10 nm) light sources, as explained further in the Discussion section.

In this study, three representative polycyclic aromatic hydrocarbons (PAHs) are doped onto mineral grains and exposed to ultraviolet radiation simulating the unfiltered Martian sunlight, under temperature and pressure conditions emulating the Martian surface environment, to quantify their photostability once uncovered on the Martian surface. Fluorescence spectroscopy is used as a sensitive indicator of the degree of PAH photodestruction over time, and emulation of fluorescence-based instrumentation for detection of Martian aromatic organics.

METHODS

Sample Preparation

Samples of mineral grains were experimentally doped with PAH as follows. Glass microscope slides were cleaned with 70% ethanol. Peridotite mineral grains of the size fraction 250–500 μm were fixed onto the glass slides in dense circles 1 cm in diameter using UN1133 all purpose clear adhesive (Everbuild, Leeds, UK), 3 spots per slide. The grains were fixed atop the patch of adhesive so UV-shielding by the glue itself is not an issue. Prior blanks tests had determined that neither peridotite grains nor the glue used to fix them to the

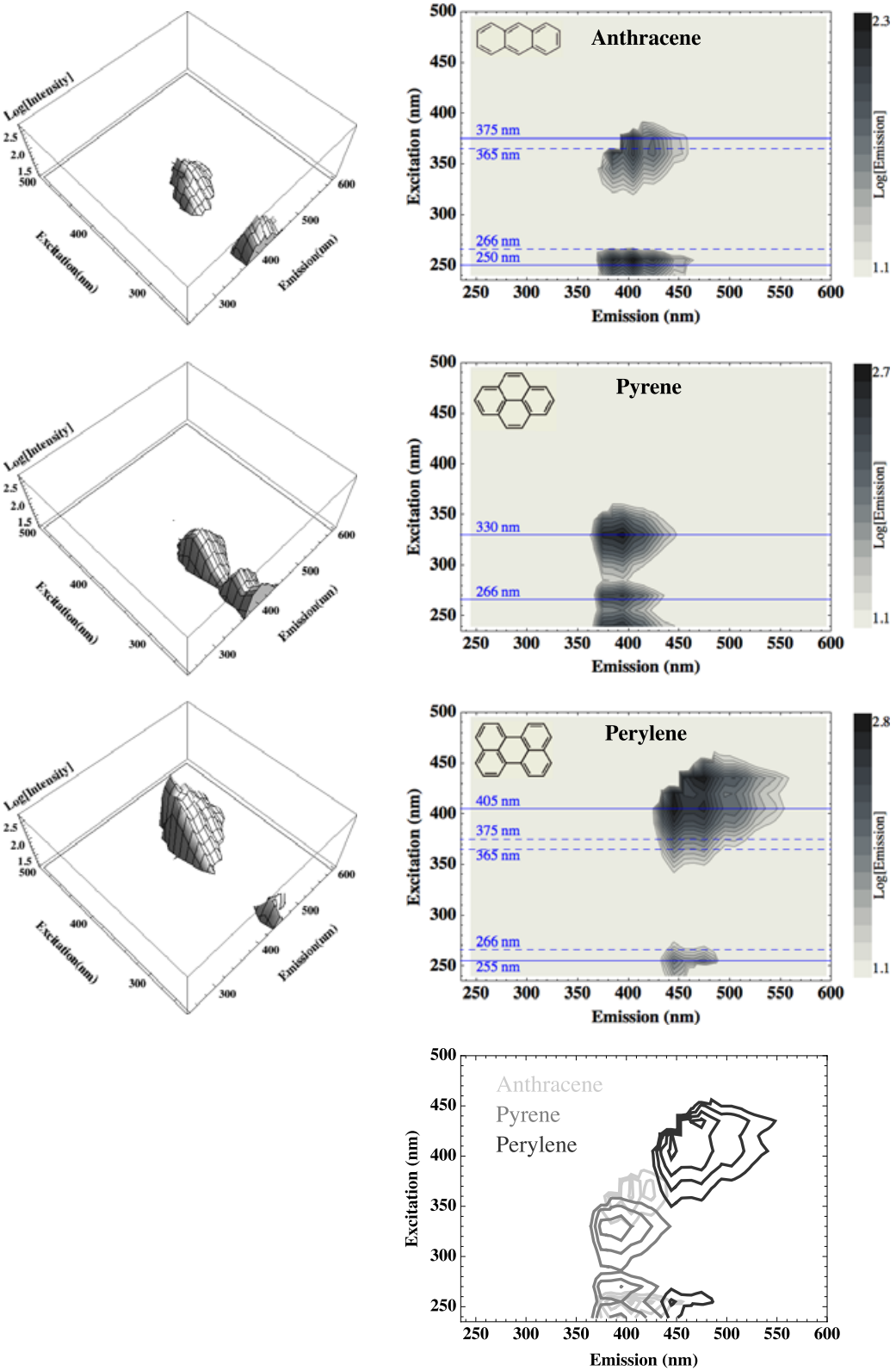

Fig. 1. Excitation-emission matrices (EEMs) displayed as both 3D terrains (left) and shaded contour maps (right) of the three representative PAHs considered here: anthracene, pyrene, and perylene. Such a display allows identification of the excitation and emission peaks of fluorescence features. Labeled solid lines show the two peak excitation wavelengths for each PAH used here, and dashed lines show the additional excitation wavelengths available from commercial LED and laser diode sources.

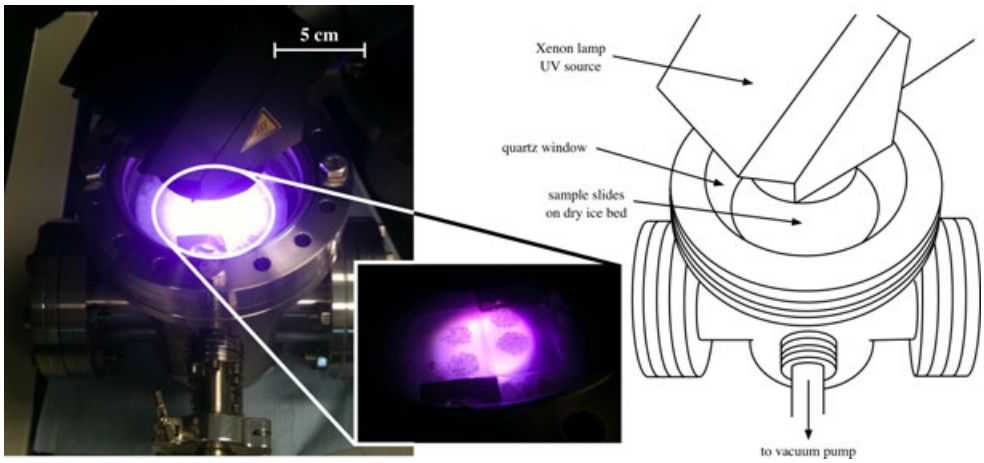

Fig. 2. Photograph and labeled diagram of the experimental set-up, showing the Mars chamber, UV light source, and samples on a bed of dry ice. The photographic inset shows a close-up of the two glass slides in the UV illumination spot. On each slide, two PAH-doped mineral grain spots are being experimentally exposed, with a third sample UV-shielded by aluminum foil as a control.

glass slides, nor the solvents methanol or methylene chloride, exhibited any detectable fluorescence of their own (data not shown here).

Analytical standard samples of three PAHs, anthracene, pyrene, and perylene, had been purchased in 1 mL ampoules (Sigma-Aldrich). Working in a fume hood, PAHs were diluted to a concentration of 40 μg/mL using the same organic solvent that the PAHs had been supplied in (anthracene: methanol; pyrene and perylene: methylene chloride). Twenty microliters of PAH was pipetted uniformly onto each of the three mineral grain spots on a glass slide, with one PAH type per slide. The solvent was allowed to rapidly evaporate in the fume hood to leave the PAH samples adhered to the surface of the peridotite grains. Each PAH was subjected to a series of five increasing exposures (see below), and in addition, a control slide of three doped grain spots was prepared, but not exposed to the Mars chamber or UV irradiation. In total, therefore, six sample slides (eighteen doped mineral spots) were prepared for each of the three PAHs.

Thus, sample preparation deposited 0.8 μg (20 μL of 40 μg/mL solution) of PAH uniformly across the peridotite grain spots. This quantity of PAH was selected for doping because pilot experimentation had determined that it produced a strong fluorescence, and without any of the three PAHs saturating the detector (see the Fluorescence Spectroscopy section). Doped mineral samples were stored overnight at room temperature before being transported to the exposure facility.

UV Exposure

UV exposures were conducted in the Mars chamber operated by the Open University, Milton Keynes, UK. Sample slides were placed two at a time onto a packed bed of dry ice (−79 °C) within the chamber, which was then sealed and evacuated to a pressure of 6 mbar. This exposed the samples to a temperature and pressure regime representative of the Martian surface. Sublimation of the dry ice occurred in the evacuated chamber, but the low pressure was maintained by the pump and the packed bed refreshed between sample runs. Illumination by a xenon lamp through a quartz top window provided the UV flux. On each glass slide, two PAH-doped mineral spots were exposed to the UV source above. The third spot was designated as control and shielded from the UV flux with aluminum foil, whilst still exposed to the low temperature and pressure regime within the chamber. The experimental set-up is shown in Fig. 2.

The xenon lamp produces a UV emission spectrum closely matching that modeled for the unfiltered sunlight incident on the Martian equatorial surface at noon during northern summer (L_s = 90°) and nominal atmospheric dust loading (Patel et al. 2002), and at a flux rate calibrated to be ten times greater, as shown in Fig. 3. This experimental protocol thus provided a faithful reproduction of both the physical conditions of the Martian surface and spectrally matched solar irradiance, while allowing accelerated experimental exposure times. One sample slide, consisting of two experimental doped grain spots and one control spot, of each PAH type was exposed within the Mars chamber for a given period of time. The experimental UV exposure times used (and their Martian equivalent exposure times) were: 6 min (1 h Mars surface equivalent), 30 min (5 Mars hours), 1 h (10 Mars hours), 2 h (20 Mars hours), and 3 h (30 h equivalent).

After timed exposure, samples were analyzed for their fluorescence response.

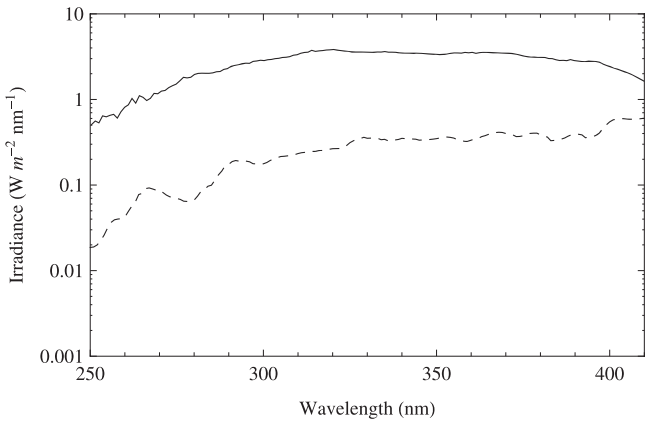

Fig. 3. The UV spectrum of simulated Martian sunlight used in these experiments (solid line) compared against the modeled solar spectrum on the Martian surface (dashed; Patel et al. 2002). The simulated Martian irradiance used here is closely spectrally matched, but at ten times higher fluence, to that expected on the Martian surface.

Fluorescence Spectroscopy

The fluorescent emission of samples was measured using a Perkin Elmer LS55 Fluorescence Spectrometer (Perkin Elmer, Cambridge, UK; L2250107). This instrument consists of a pulsed xenon arc lamp light source, excitation and emission scanning monochromators, and a photomultiplier tube (PMT) detector.

A remote fiber-optic accessory (Perkin Elmer; L2250144) was used to measure fluorescence from the solid surface of the doped mineral samples. This attachment uses bifurcated fused silica fiber optics to pass excitation light from the xenon source to the sample surface, and also fluorescent emission from the sample to the detector, down two halves of the same cable. The head of the fiber-optic cable was positioned 8 mm above the surface of the mineral grains; the distance that had been found to be optimal for surface fluorescence measurements. A blackout curtain was used to isolate the sample and fiber-optic head from ambient light in the laboratory. Precise targeting of the fiber-optic attachment onto the mineral spot was achieved with the selection of the visible wavelength of 500 nm (green), before changing to the short wavelength excitation light.

FL WinLab software (Perkin Elmer; B8011050) was used to control the spectrometer, setting the desired excitation wavelength and recording the emission spectrum over a set wavelength range. Emission spectra between 240 and 600 nm were recorded at 50 nm/min scan speed with an excitation slit width of 8 nm and emission slit width of 5 nm. Raw data were processed using analysis code written by the first author in Mathematica 8 (Wolfram).

The fluorescent response from each doped sample was measured at two peak excitation wavelengths appropriate to the PAH. Figure 1 shows the EEM generated for each of the three PAHs, with the corresponding peak excitation wavelengths indicated with dashed lines. In addition, fluorescence was measured from excitation wavelengths relevant to available LEDs or laser diodes that could provide excitation light for a fluorescence-based instrument. The available wavelengths relevant to excitation of anthracene, pyrene, or perylene are 266 nm (achieved by frequency-doubling a green 532 nm laser), 365, 375, and 405 nm. The excitation wavelengths selected for the three PAHs are listed in Table 1.

Each PAH-doped peridotite grain spot was measured three times with repositioning of the fiber-optic head in a triangular pattern over the spot, as described above. Thus, for each excitation wavelength of interest, both independent experimental samples were measured in triplicate, and the control sample was also measured in triplicate.

The time between deposition of the PAH samples, UV exposure, and fluorescence analysis was no longer than 72 h. Pilot experimentation had verified that loss of PAHs to volatilization at room temperature and pressure did not occur over this time frame.

RESULTS

Figure 4, left column, shows the fluorescence emission spectra of the three PAHs considered here, anthracene (top row), pyrene (middle), and perylene (bottom). All spectra have been plotted on the same emission wavelength and intensity scale to allow comparison. Each spectrum has been cropped to exclude the scattered excitation light and its harmonics, and represents an average over the three unexposed control samples, each measured in triplicate. In each case, the blue emission spectrum corresponds to the shorter wavelength excitation maximum, and the red spectrum that induced by the longer wavelength excitation used. These two peak excitation wavelengths for each PAH are indicated with solid horizontal lines in the EEMs displayed in Fig. 1, and are listed in bold in Table 1. The vertical shaded bars in Fig. 4 indicate the peak emission wavelength, ± 1 nm, and are the range of values over which the fluorescent emission is averaged.

The right column of Fig. 4 shows the peak fluorescence intensity measured for the control samples after increasing periods exposed to Martian surface temperature and pressure (but not UV irradiation), normalized to the mean of the three control samples unexposed to simulated Martian conditions, and plotted on a log scale (i.e., $\log[N/N_0]$). Errors bars, calculated as plus and minus the standard error of the measurements,

Table 1. Excitation wavelengths used for the three PAH samples.

Anthracene	**250 nm**			365 nm	**375 nm**	
Pyrene		**266 nm**	**330 nm**			
Perylene	**255 nm**	266 nm		365 nm	375 nm	**405 nm**

Wavelengths listed in **bold** correspond to the peak excitation, as determined from the EEMs shown in Fig. 1. Other wavelengths correspond to those available from commercial LED and laser diode sources.

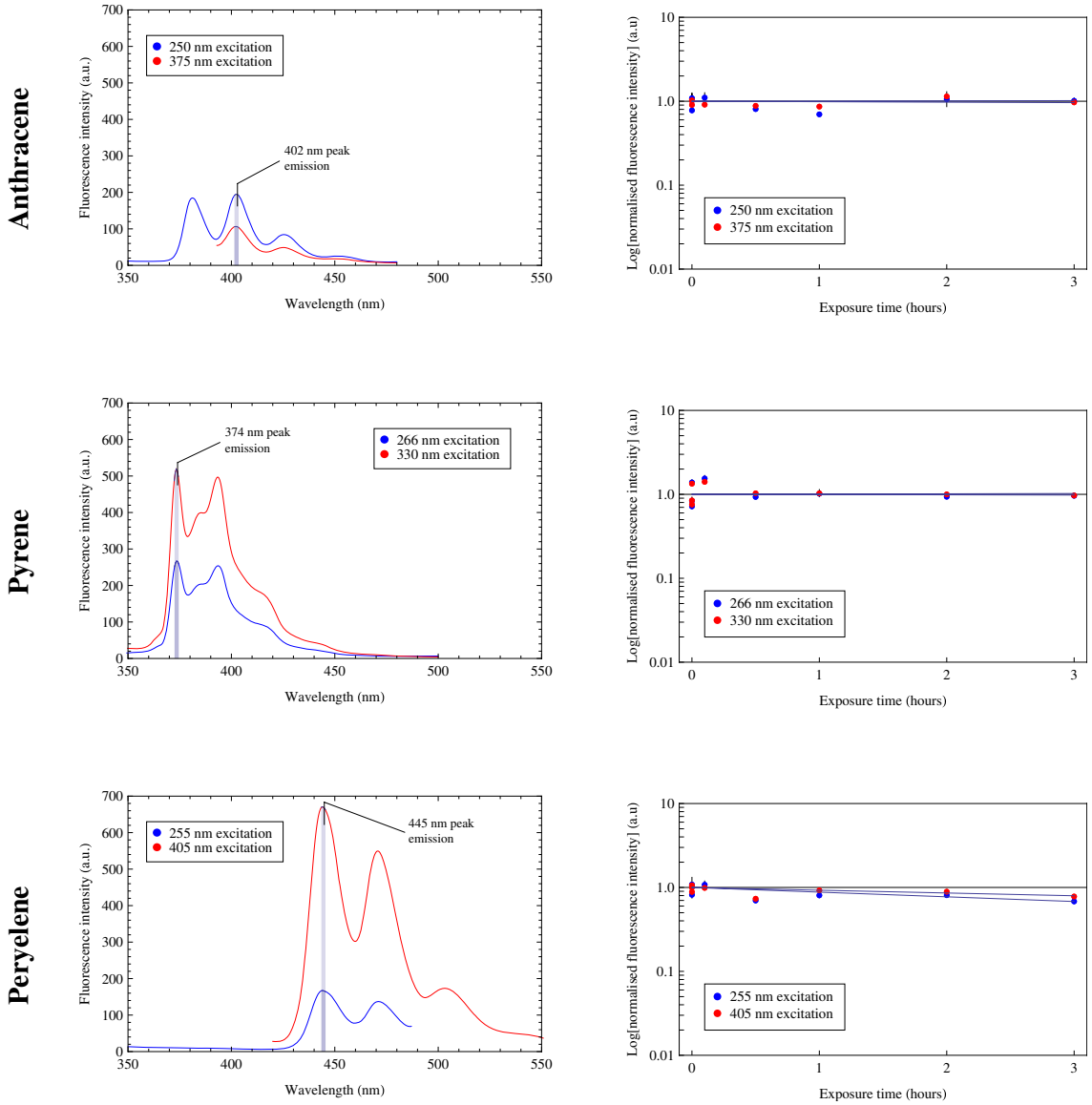

Fig. 4. (left column) Fluorescence emission spectra averaged over all three unexposed control samples, measured in triplicate. Blue spectra are recorded from the short peak excitation wavelength and red spectra from the longer peak excitation wavelength used, as indicated in Fig. 1 and Table 1; (right column) Fluorescence emission intensity from the control samples exposed to the simulated Martian surface temperature and pressure regime, but shielded from the UV flux.

are plotted but on the log scale are generally obscured by the data points themselves. Fluorescence measurements from both short and long wavelength excitation (see left column) are indicated with blue and red color-coded data points, respectively. These controls have been exposed to the simulated temperature and pressure regime of the Martian surface for the indicated period, but not the ultraviolet illumination (shielded beneath aluminum foil). It can be seen that, as expected, the anthracene and pyrene deposited samples show no detectable reduction after up to 3 h exposure to 6 mbar pressure at −79°C. The perylene control samples do,

however, exhibit a slight decrease. The gradient of this trend, fitted to fluorescence measurements from both excitation wavelengths, is −0.00445 (SE = 0.00114). This trend is accounted for in the analysis of the UV-exposed experimental samples of perylene, as explained below.

Figure 5 displays the change in fluorescence emission intensity as a function of the Martian-equivalent hours of UV exposure under simulated Martian conditions. These Martian-equivalent exposure times are calculated for an equatorial region at local noon during northern summer, with a nominal atmospheric dust loading (using the model reported in Patel et al. 2002), and will be covered further in the Discussion section. As with Fig. 4, the log fluorescence scale is normalized to the averaged emission recorded from the three controls (each measured in triplicate) unexposed to UV or Martian environmental conditions. Data are presented for two independent experimental samples, each measured in triplicate, and each analyzed at two peak excitation wavelengths (see Fig. 4). Samples and excitation wavelengths are coded as explained in the figure caption. A best-fit trend line is calculated for each of the four data sets measured for each PAH. The mean of these fitted trend lines is displayed in Fig. 5, along with the range defined by the standard error of these estimates. Table 2 summarizes the parameters of these fitted trend lines of PAH degradation. As explained above, the perylene control samples show a slight decrease in fluorescence signal with duration exposed to the low pressure and low temperature experimental conditions. The fitted exponent for perylene degradation with UV exposure shown in Table 2 has had this control exponent subtracted, and the standard errors have been summed.

Measurements of the decrease in fluorescence intensity were also made at wavelengths other than the peak excitations for the different PAHs, appropriate to the emission wavelengths of available LED and laser diode light sources. These additional wavelengths were 365 nm for anthracene and 266, 265, 375 nm for perylene (the excitation peak of pyrene fortuitously lies on the available laser diode wavelength of 266 nm), as illustrated in Fig. 1 with dashed lines. Figure 6 displays the results of degrading fluorescence signal with period of UV exposure on the Martian surface for these excitation wavelengths. As with Fig. 4, the mean trend line fitted to the data is shown, along with the region defined by the standard error of the results.

Table 3 summarizes the parameters of these fitted trend lines of PAH fluorescent signal loss, when excited at these alternative wavelengths. Again, the decrease in signal from perylene control samples has been removed from these perylene fitted exponents, and the standard errors summed.

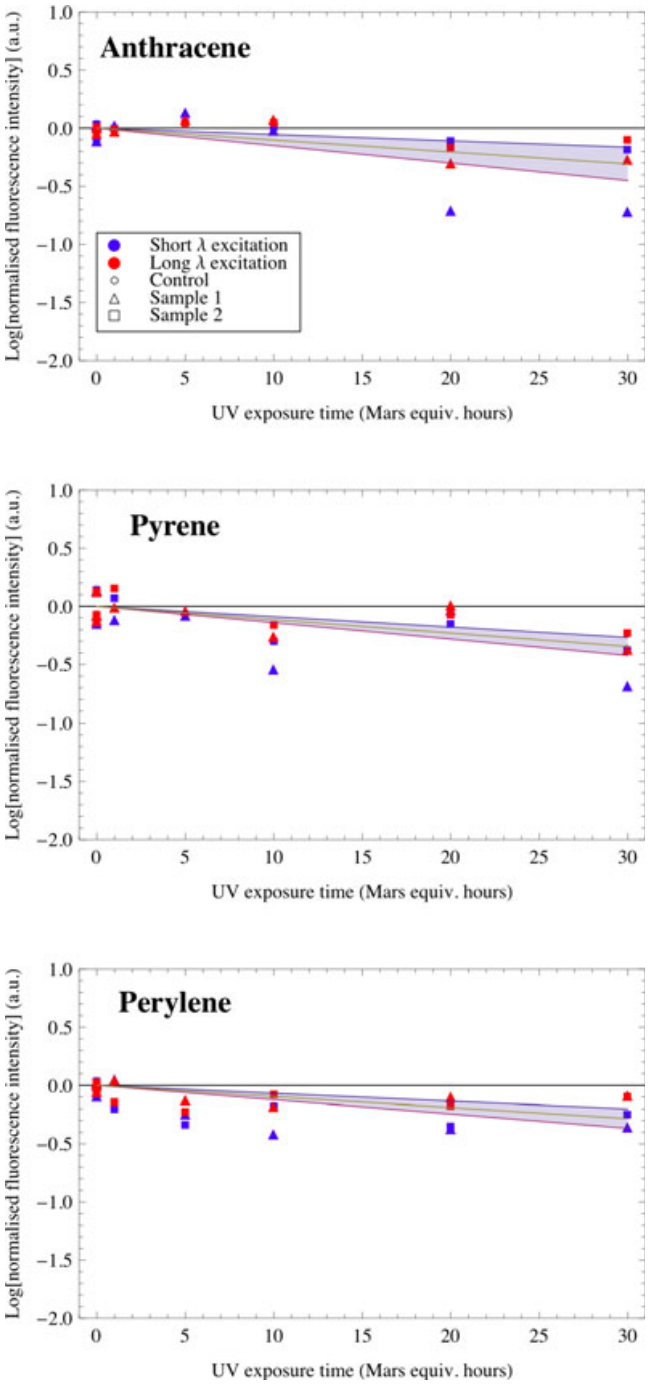

Fig. 5. Plots of the change in fluorescence emission intensity (Log_{10} scale) against the duration of Mars equivalent UV exposure. The fluorescence scale is normalized to the averaged emission recorded from the unexposed controls. For each PAH sample, blue data points indicate the shorter peak excitation wavelength and red data points, the longer excitation wavelength used. Each data point is the average emission of a sample measured in triplicate, with error bars plotted as the standard error of the mean and generally obscured by the data points themselves. Circles: unexposed control samples; triangles: first exposed sample; squares: second exposed sample.

Table 2. The calculated UV-degradation rates of PAH fluorescence, listing the mean exponent of the fitted trends to the four data sets and the standard error of this measure.

	Fitted exponent	Standard error	Half-life (Mars-equivalent hours)	Time to 10% remaining signal (hours)
Anthracene	−0.01023	±0.00478	29.4	97.8
Pyrene	−0.01150	±0.00259	26.2	86.9
Perylene *	−0.00501	±0.00391	60.0	199.4

Also shown are calculations of the half-life of decreasing PAH fluorescence, and the total duration of exposure required to diminish fluorescent emission to 10% of the initial intensity. These times are based on the modeled equatorial noontime flux during northern summer, and so actual persistence times will be longer, as explained in the Discussion section. *The fitted exponent displayed here for perylene has already had the decreasing trend observed in the control samples (Fig. 4) removed, and the standard errors summed.

DISCUSSION

Organic molecules are expected on the Martian surface, even in the absence of biology, through compounds synthesized by astrochemistry and delivered by meteoritic and cometary infall, as well as remnants of in situ Martian prebiotic chemistry. Many of these prebiotic molecular targets contain aromatic moieties and so exhibit fluorescent emission when excited. A large class of such compounds are the polycyclic aromatic hydrocarbons, PAHs, which are found in abundance in the interstellar medium, within carbonaceous chondrite meteorites, and also in meteorite samples of the Martian surface such as ALH 84001.

Organic compounds are yet to be detected on the Martian surface, and it has been proposed to exploit the fluorescence emission from molecules with aromatic moieties as a means to survey for assemblages of organic molecules on Mars. Such a fluorescence-based surveying instrument would identify promising target locations for the first detection of organics with other more discriminatory instruments, and possibly also reveal niches of relic life.

The intense ultraviolet component of unfiltered Martian sunlight, however, would be expected to photobleach fluorescence and ultimately photolyse and destroy exposed target compounds (Cockell et al. 2005; ten Kate et al. 2005, 2006; Garry et al. 2006; Peeters et al. 2009; Stalport et al. 2009). Organic molecules may persist on Mars, shielded from solar UV inside rocks or in the subsurface, but will face degradation as soon as they become exposed to the unfiltered sunlight. After uncovering fresh Martian samples, with a rock abrasion tool or subsurface drill, for example, there is therefore a limited window of opportunity to survey for the presence of fluorescent organic compounds and decide whether to employ more discriminatory, but resource-limited, instruments. The crucial question, therefore, is what is the photostability of these PAH target molecules—what is the rate of loss of the fluorescence signal once exposed to Martian sunlight?

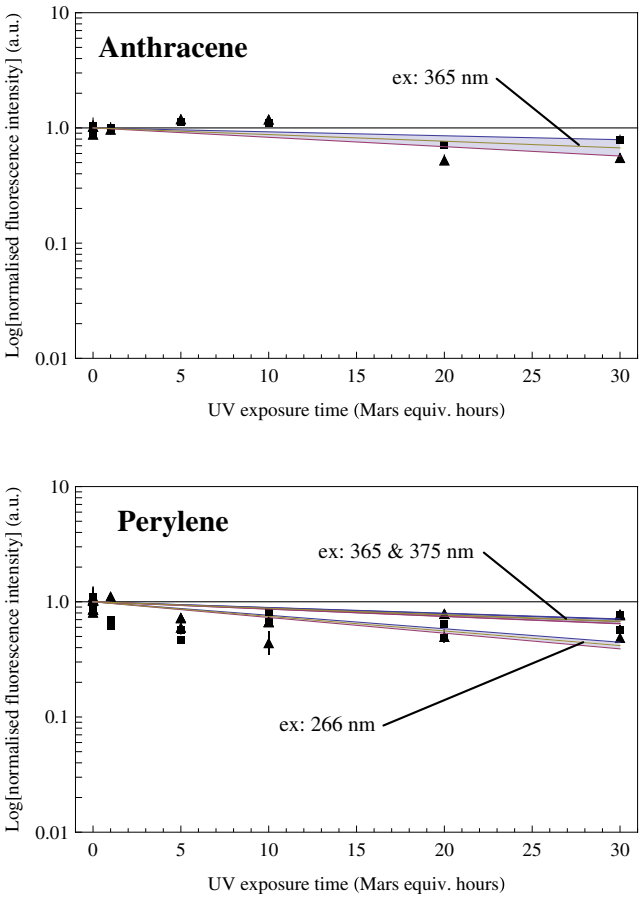

Fig. 6. Plots of the change in fluorescence emission intensity (Log_{10} scale) against the duration of Mars equivalent UV exposure when anthracene and perylene are excited at additional wavelengths corresponding to available LED and laser diode light sources. The fluorescence scale is normalized to the averaged emission recorded from the unexposed controls. Each data point is the average emission of a sample measured in triplicate, with error bars plotted as the standard error of the mean and generally obscured by the data points themselves. Circles: unexposed control samples; triangles: first exposed sample; squares: second exposed sample.

PAH Fluorescence

The study reported here addresses this key unknown. Three representative PAH compounds, anthracene, pyrene, and perylene (3-, 4-, and 5-ring PAHs, respectively, as shown in Fig. 1), were selected and the remaining fluorescence signal quantified at a variety of

Table 3. The calculated UV-degradation rates of PAH fluorescence, as measured at the indicated excitation wavelength of relevance to commercially available LED and laser diode light sources.

	Fitted exponent	Standard error	Half-life (Mars-equivalent hours)	Time to 10% remaining signal (hours)
Anthracene; 365 nm	−0.00577	±0.00237	52.2	173.3
Perylene; 266 nm*	−0.00822	±0.00210	36.6	121.7
Perylene; 365 nms*	−0.00131	±0.00178	229.9	763.7
Perylene; 375 nm*	−0.00118	±0.00181	254.2	844.6

The table lists the mean exponent fitted to the data recorded from both experimental samples, and the standard error of this measure. Also shown are calculations of the half-life of decreasing PAH fluorescence, and the total duration of exposure required to diminish fluorescent emission to 10% of the initial intensity. These times are based on the modeled equatorial noontime flux during northern summer, and so actual persistence times will be longer, as explained in the Discussion section. *The fitted exponents displayed here for perylene have already had the decreasing trend observed in the control samples (Fig. 4) removed, and the standard errors summed.

excitation wavelengths after increasing periods of exposure to simulated Martian UV flux under emulated surface conditions of cold and low pressure atmosphere. These particular PAH compounds were chosen because they are common components of the organic inventory within carbonaceous chondrites and are also fluorescent, making them promising targets for detection on Mars.

The fluorescence spectra taken of the control samples (three samples of each PAH, each measured in triplicate) shown in Fig. 4 were used to normalize the remaining signal plotted in Figs. 5 and 6. From the intensity of the fluorescence peaks shown in Fig. 4, left column, it can be seen that perylene adhered onto peridotite grains is approximately 3.5 times more intrinsically fluorescent than anthracene, and 30% more intense than pyrene, as measured at their peak excitation and emission. It is also worth noting that perylene, the largest PAH considered here, comprised of 5 aromatic rings (see Fig. 1), exhibits both the longest peak excitation and emission wavelength.

PAH Volatilization

The plots in the right-hand column of Fig. 4 track the fluorescence signal over 3 h of exposure to the simulated Martian surface conditions of 6 mbar atmospheric pressure at −79 °C, but shielded from UV radiation. Whilst anthracene and pyrene samples are very stable over this period, perylene does show a slight loss in signal. The effect of this decrease over time is simple to remove from the UV-exposed experimental perylene sample data, as described in the Results section. Whilst this control correction does increase the standard error of the estimate, it is still clear that the perylene fluorescent signal can persist for a significant duration once exposed on the Martian surface, as discussed in greater depth below.

This observed fluorescence signal decrease in the perylene control samples unexposed to UV is believed to be due to the slow volatilization of the small organic molecules off the surface of the mineral grains under low atmospheric pressure. The fact that out of all the UV shielded control samples perylene shows the most reduction is a surprise. Perylene has the highest molecular weight of the three representative PAHs tested here, and so would be expected to be the least volatile. However, such low molecular weight aromatics are found in abundance in carbonaceous chondrite meteorites, after very long-term exposure to the vacuum of space, and so their long-term stability in the environmental conditions of the Martian surface is not under question. Inside carbonaceous meteorites, the prevalence of intramolecular bonds within the complex assemblage of organics, including much larger and refractory molecules and a cross-linked matrix of macromolecules making up the "kerogen-like" material (Botta and Bada 2002), would thus serve to stabilize the lower molecular weight species against volatilization. In this experimental set-up, PAHs were adhered onto mineral grains from pure solution; a necessary simplification to allow quantification of the degradation rate of each compound. In the Martian environment, aromatic prebiotic compounds, either synthesized in situ or the products of astrochemistry delivered aboard meteorites, would be present in much more complex, mixed assemblages, and so be much less susceptible to volatilization than the pure samples considered here.

PAH Photostability

In any case, the UV degradation rates quantified by excitation at the peak wavelengths, plotted in Fig. 5 and the fitted exponents summarized numerically in Table 2, show a clear result. All three representative PAH compounds considered here are demonstrated to exhibit a detectable degradation in fluorescent signal over the 30 h of simulated Martian surface UV exposure. The half-life of this declining fluorescence ranges from about 25 to 60 h. The photostabilities of anthracene and pyrene are measured here to be very similar, and this result is corroborated by Jochims et al. (1999) who experimentally

determined a photostability index for a range of PAHs under conditions of the interstellar medium, and also found anthracene and pyrene to exhibit near-identical rates. By way of comparison, Ram and Anastasio (2009) experimentally determined the photostability of PAHs exposed to simulated sunlight in arctic snow. They calculated that in surface snow at midday on the summer solstice at Summit, Greenland, the photodegradation half-life of pyrene is just over 40 min. Whilst the UV flux at Greenland is less than on the Martian surface, Ram and Anastasio (2009) irradiated at warmer temperatures (−2.4 to −11 °C) and with the PAH molecules within water ice (not adhered on dry mineral grains, as with this current study) and so they were additionally subject to degradation from hydroxyl radicals.

Multiple samples were irradiated to ensure a high degree of accuracy on these fitted trend lines. If these measured trends do continue to higher total UV doses, pyrene emission is down to only 10% of its initial value after around 90 h of Martian sunlight, and perylene after around 200 h.

These results on degradation rates of PAHs under UV irradiation and simulated Martian surface environmental conditions are comparable to similar previous studies on the photostability of organic molecules on Mars. ten Kate et al. (2005) subjected thin films of amino acids to Mars-like UV flux levels and discovered that the photodecomposition half-life of glycine is 22 ± 5 h and that of D-alanine is 3 ± 1 h. The difference between the degradation of these two amino acids is believed to be due to the rate-limiting step of the free radical chemistry driven by absorption of a UV photon (ten Kate et al. 2005). However, when these room-temperature experiments were repeated simulating a Martian surface temperature of 210 K (−63 °C), as this current study has done, the UV destruction rate for glycine were found to decrease by a factor of 7, as expected from slower reaction kinetics at low temperatures (ten Kate et al. 2006). Stalport et al. (2009) exposed carboxylic acids to Mars-like ultraviolet irradiation under cold conditions of −55 °C. They found that the mass loss of mellitic acid reached 50% after approximately 25 h exposure. Benzoic and oxalic acids were discovered to be much more photosensitive, exhibiting mass loss half-lives of 0.8 ± 0.2 h and 1.8 ± 0.5 h, respectively. Schuerger et al. (2008) deposited ATP onto a simulated spacecraft surface and exposed to Martian surface conditions and UV flux and found a degradation half-life of around 40 Martian sols at −80 °C. Looking at more complex, exclusively biological molecules, Cockell et al. (2005) found that autofluorescence from the photosynthetic pigments (phycobiliproteins and chlorophyll a) of the cyanobacterium Chroococcidiopsis sp. 029 was diminished to 1% by 4 h of exposure to Martian UV flux.

Illuminating the samples with the appropriate excitation peak wavelength is the most sensitive fluorescence method for assessing PAH degradation with UV exposure, but this study also analyzed fluorescence emission excited by other, non-optimal, wavelengths for the PAHs. The design of an instrument for the detection of fluorescent organic molecules may dictate the use of a single excitation wavelength that is not optimal for all potential targets. However, even at a suboptimal wavelength for an organic molecule target, fluorescence may still be detectable if the excitation light source is intense, such as from a laser diode or LED at close range. The available LED or laser diode wavelengths examined were 266, 365, 375, and 405 nm, and it is worth stressing at this point that each of the PAHs studied here are optimally excited at an available wavelength (anthracene, 375 nm; pyrene, 266 nm; perylene, 405 nm; as shown in Table 1).

Decrease in the fluorescent signal may not be uniform across the emission feature, and it is important to verify the signal decrease from the other, non-optimal, excitation wavelengths for each PAH. Figure 6 and Table 3 display the results on the decrease in fluorescence when excited at these alternative wavelengths. More variability in the degradation rate is seen with these non-optimal excitation wavelengths, with calculated half-lives ranging from 37 h (perylene excited at 266 nm) to over 250 h (perylene excited at 375 nm). This indicates that the degradation of fluorescence from UV exposure is not uniform across the excitation-emission parameter space, with some regions of the fluorescent feature diminishing faster than others. Importantly, however, even exciting at a wavelength non-optimal for these PAHs the UV degradation rates are low enough that there is a significant window of opportunity for detection after exposure of the material to Martian sunlight.

The resounding result from these experimental is that although a decrease in the fluorescence signal of all three tested PAHs is detectable after 30 h of simulated exposure on the Martian surface, this signal decrease is not overwhelming over time scales of relevance to the surface operations of a robotic rover. If a rover is able to expose fresh material on the surface, either by rock abrasion tool or subsurface drill, it has a window of opportunity of at least 10 h to survey for fluorescence from any native organics.

Diurnal Flux

These Mars-equivalent exposure times were calculated for equatorial midday during northern summer with a nominal atmospheric dust loading (using the model reported in Patel et al. 2002). As the solar

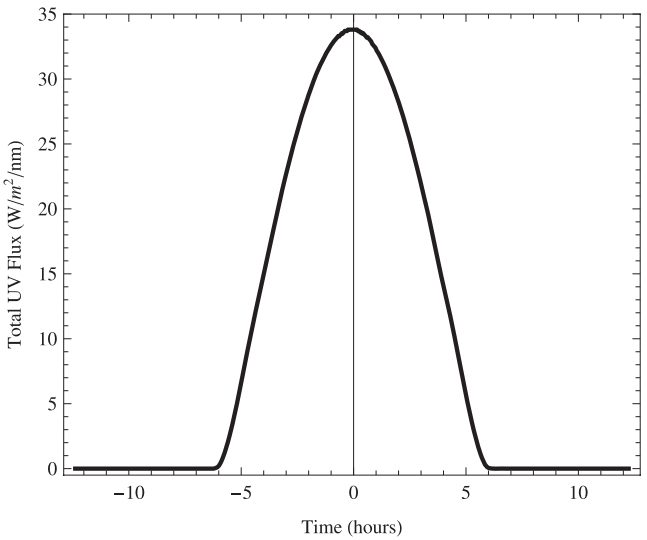

Fig. 7. Plot of the diurnal cycle in UV flux rate calculated for the Martian surface (by the atmospheric transmission model reported in Patel et al. 2002) at an equatorial latitude and during northern summer with an atmospheric opacity due to dust loading of 0.2, representing a realistic nominal case for exposure experiments. The time axis is shown in units of hours from local noon.

zenith angle varies over the course of a day on Mars, the actual instantaneous UV exposure rate will generally be less than this. Consequently, the number of Martian sols before PAH fluorescence diminishes to 50% or 10% is not simply a twelfth of the number of hours listed in Tables 2 and 3. Figure 7 plots the instantaneous UV flux rate at an equatorial latitude and during northern summer with an atmospheric opacity due to dust loading of 0.2, representing a realistic nominal case for exposure experiments.

The UV dose rate can be seen to peak at around 33 W/m^2/nm at local noon, but rapidly drops off earlier in the morning and later in the afternoon. Integrating across a complete diurnal cycle, with the instantaneous UV flux changing as shown in Fig 7, defines the total Mars daily UV dose (200–400 nm) to be around 872,000 J/m^2 (to 3 significant figures) (Patel et al. 2002, 2004).

This allows the calculation of a more meaningful time conversion for exposures on the Martian surface. Every Mars equivalent hour of UV irradiation at equatorial summer noontime flux (corresponding to 6 min of experimental irradiation in this set-up), as listed in Tables 2 and 3, is equivalent to 0.16 sols of the total flux averaged over the diurnal cycle.

This relationship between experimental exposure doses and actual UV fluxes over the day-night cycle on Mars is important to appreciate and account for in laboratory studies of the effects of unfiltered Martian sunlight.

The half-lives of fluorescent signal degradation of the PAHs anthracene, pyrene and perylene listed in Table 2, ranging between around 25 and 60 h of irradiation at noontime flux levels, thus actually equate to half-lives between 4 and 9.6 Martian sols when the full diurnal cycle is considered. It is therefore comfortably within the operational scope of robotic rovers to uncover caches of Martian organics, previously shielded either in the subsurface regolith or within surface rocks, and survey for indicative fluorescence before the freshly exposed compounds are photodegraded. Such an exploratory program would obviously be most effective if drilling by day, and then testing the uncovered material for a fluorescent signal at dusk or early the following morning. This strategy optimizes both the persistence of exposed organic molecules and the detectable fluorescence signal in low ambient light.

A more complete simulation of the situation will involve cycling of UV intensity to more faithfully recreate Martian daylight over several sols, as well as diurnal temperature cycles and consequent cycles of water frosting and sublimation, to study these additional parameters on PAH photostability.

CONCLUSIONS

Ultimately, detection of fluorescence from organic compounds near the Martian surface depends on multiple factors, including the localized fluorophore concentration, target range, intensity of the excitation light source, and sensitivity of the spectrometer or imaging instrument. It is clear from this experimental program, however, that over a time scale of relevance to operations of a robotic mission on the Martian surface, these three representative PAHs do not experience substantial degradation of their detectable fluorescence signal. Irradiated on mineral grains under Martian surface conditions and then tested at their peak fluorescence excitation wavelength, anthracene, pyrene, and perylene were all found to exhibit a UV-degradation half-life of between around 25 and 60 h at northern summer noontime flux levels, which equates to between 4 and 9.6 Martian sols when the full diurnal cycle is considered.

The nature of the changing UV flux over the diurnal cycle is an important consideration to take into account when relating the results of laboratory UV irradiation experiments to the reality of the time-variable UV environment of the Martian surface.

The results presented here are thus supportive of rover-mounted fluorescence-based instruments for surveying for the presence of prebiotic organic molecules such as PAHs.

Acknowledgments—The research leading to these results has received funding from the European Community's Seventh Framework Programme (FP7/2007–2013) under grant agreement no 241523 PRoViScout. LRD is supported by the UCL Institute of Origins Post-Doctoral Research Associateship. MRP is supported by funding from the Science and Technology Facilities Council (STFC).

Editorial Handling—Dr. A. J. Timothy Jull

REFERENCES

Alberts J. and Takács M. 2004. Total luminescence spectra of IHSS standard and reference fulvic acids, humic acids and natural organic matter: Comparison of aquatic and terrestrial source terms. *Organic Geochemistry* 35:243–256.

Aubrey A., Chalmers J et al. 2008. The Urey Instrument: An advanced in situ organic and oxidant detector for Mars exploration. *Astrobiology* 8:583–595.

Becker L., Popp B. et al. 1999. The origin of organic matter in the Martian meteorite ALH84001. *Advances in Space Research* 24:477–488.

Benner S. A., Devine K. G. et al. 2000. The missing organic molecules on Mars. *Proceedings of the National Academy of Sciences* 97:2425–2430.

Biemann K., Oro J. et al. 1977. The search for organic substances and inorganic volatile compounds in the surface of Mars. *Journal of Geophysical Research* 82:4641–4658.

Botta O. and Bada J. 2002. Extraterrestrial organic compounds in meteorites. *Surveys in Geophysics* 23:411–467.

Botta O., Martins Z. et al. 2008. Polycyclic aromatic hydrocarbons and amino acids in meteorites and ice samples from LaPaz Icefield, Antarctica. *Meteoritics & Planetary Science* 43:1465–1480.

Clemett S. J., Dulay M. T. et al. 1998. Evidence for the extraterrestrial origin of polycyclic aromatic hydrocarbons in the Martian meteorite ALH84001. *Faraday Discussions* 109:417–436.

Cockell C., Schuerger A. et al. 2005. Effects of a simulated Martian UV flux on the Cyanobacterium, Chroococcidiopsis sp. 029. *Astrobiology* 5:127–140.

Cory R. and McKnight D. 2005. Fluorescence spectroscopy reveals ubiquitous presence of oxidized and reduced quinones in dissolved organic matter. *Environmental Science & Technology* 39:8142–8149.

Dartnell L. R., Storrie-Lombardi M. C. et al. 2010. Complete fluorescent fingerprints of extremophilic and photosynthetic microbes. *International Journal of Astrobiology* 9:245–257.

Dartnell L., Storrie-Lombardi M. et al. 2011. Degradation of cyanobacterial biosignatures by ionizing radiation. *Astrobiology* 11:997–1016.

Edgett K., Ravine M., et al. 2009. The Mars Science Laboratory (MSL) Mars hand lens imager (MAHLI) flight instrument (abstract #1197). 40th Lunar and Planetary Science Conference. CD-ROM.

Ehrenfreund P. and Charnley S. 2000. Organic molecules in the interstellar medium, comets, and meteorites: A voyage from dark clouds to the Early Earth. *Annual Review of Astronomy and Astrophysics* 38:427–483.

Ellery A. and Wynn-Williams D. 2003. Why Raman spectroscopy on Mars? A Case of the Right Tool for the Right Job. *Astrobiology* 3:565–579.

Evans-Nguyen T., Becker L. et al. 2008. Development of a low power, high mass range mass spectrometer for Mars surface analysis. *International Journal of Mass Spectrometry* 278:170–177.

Flynn G. 1996. The delivery of organic matter from asteroids and comets to the early surface of Mars. *Earth, Moon, and Planets* 72:469–474.

Garry J., ten Kate I. et al. 2006. Analysis and survival of amino acids in Martian regolith analogs. *Meteoritics & Planetary Science* 41:391–405.

Gibson E., McKay D. et al. 2001. Life on Mars: Evaluation of the evidence within Martian meteorites ALH84001, Nakhla, and Shergotty. *Precambrian Research* 106:15–34.

Goesmann F., Becker L., et al. 2009. MOMA, the search for organics of the ExoMars mission. *EPSC Abstracts* 4: EPSC2009-2624.

Gorevan S., Myrick T. et al. 2003. Rock abrasion tool: Mars exploration Rover mission. *Journal of Geophysical Research* 108:8068.

Griffiths A., Coates A. et al. 2008. Enhancing the effectiveness of the ExoMars PanCam instrument for astrobiology. *Geophysical Research Abstracts* 10:EGU2008–A09486.

Herbst E. and Van Dishoeck E. 2009. Complex organic interstellar molecules. *Annual Review of Astronomy and Astrophysics* 47:427–480.

Howerton S., Goodpaster J. et al. 2002. Characterization of polycyclic aromatic hydrocarbons in environmental samples by selective fluorescence quenching. *Analytica Chimica Acta* 459:61–73.

Hua B., Dolan F. et al. 2007. Water-source characterization and classification with fluorescence EEM spectroscopy: PARAFAC analysis. *International Journal of Environmental Analytical Chemistry* 87:135–147.

JiJi R., Cooper G. et al. 1999. Excitation-emission matrix fluorescence based determination of carbamate pesticides and polycyclic aromatic hydrocarbons. *Analytica Chimica Acta* 397:61–72.

Jochims H. W., Baumgärtel H. et al. 1999. Structure-dependent photostability of polycyclic aromatic hydrocarbon cations: Laboratory studies and astrophysical implications. *The Astrophysical Journal* 512:500–510.

Jorge Villar S. and Edwards H. 2006. Raman spectroscopy in astrobiology. *Analytical and Bioanalytical Chemistry* 384:100–113.

ten Kate I. 2010. Organics on Mars? *Astrobiology* 10:589–603.

ten Kate I., Garry J. et al. 2005. Amino acid photostability on the Martian surface. *Meteoritics & Planetary Science* 40:1185–1193.

ten Kate I., Garry J. et al. 2006. The effects of Martian near surface conditions on the photochemistry of amino acids. *Planetary and Space Science* 54:296.

Ko E., Lee C. et al. 2003. Monitoring PAH-contaminated soil using laser-induced fluorescence (LIF). *Environmental Technology* 24:1157–1164.

Mahaffy P. 2008. Exploration of the habitability of Mars: Development of analytical protocols for measurement of organic carbon on the 2009 Mars Science Laboratory. *Space Science Reviews* 135:255–268.

Marshall C., Edwards H. et al. 2010. Understanding the application of Raman spectroscopy to the detection of traces of life. *Astrobiology* 10:229–243.

Martins Z. 2011. Organic chemistry of carbonaceous meteorites. *Elements* 7:35–40.

Martins Z., Botta O. et al. 2008. Extraterrestrial nucleobases in the Murchison meteorite. *Earth and Planetary Science Letters* 270:130–136.

McKay D., Gibson E. et al. 1996. Search for past life on Mars: Possible relic biogenic activity in Martian meteorite ALH84001. *Science* 273:924–930.

Moores J., Smith P. et al. 2007. The shielding effect of small-scale Martian surface geometry on ultraviolet flux. *Icarus* 192:417–433.

Muller J. P., Storrie-Lombardi M., et al. 2009. WALI—Wide angle laser imaging enhancement to ExoMars PanCam: A system for organics and life detection. *EPSC Abstracts* 4:EPSC2009-2674-2001.

Nadeau J., Perreault N. et al. 2008. Fluorescence microscopy as a tool for in situ life detection. *Astrobiology* 8:859–874.

Okon A. B.2010. Mars Science Laboratory Drill. Proceedings of the 40th Aerospace Mechanisms Symposium. pp. 1–16.

Patel M., Zarnecki J. et al. 2002. Ultraviolet radiation on the surface of Mars and the Beagle 2 UV sensor. *Planetary and Space Science* 50:915–927.

Patel M., Christou A. et al. 2004. The UV environment of the Beagle 2 landing site: Detailed investigations and detection of atmospheric state. *Icarus* 168:93–115.

Patra D. and Mishra A. 2001. Investigation on simultaneous analysis of multicomponent polycyclic aromatic hydrocarbon mixtures in water samples: A simple synchronous fluorimetric method. *Talanta* 55:143–153.

Peeters Z., Quinn R. et al. 2009. Habitability on planetary surfaces: Interdisciplinary preparation phase for future Mars missions. *International Journal of Astrobiology* 8:301–315.

Pierazzo E. and Chyba C. F. 1999. Amino acid survival in large cometary impacts. *Meteoritics & Planetary Science* 34:909–918.

Pizzarello S. 2006. The chemistry of life's origin: A carbonaceous meteorite perspective. *Accounts of Chemical Research* 39:231–237.

Quinn R. and Zent A. 1999. Peroxide-modified titanium dioxide: A chemical analog of putative Martian soil oxidants. *Origins of Life and Evolution of Biospheres* 29:59–72.

Ram K. and Anastasio C. 2009. Photochemistry of phenanthrene, pyrene, and fluoranthene in ice and snow. *Atmospheric Environment* 43:2252–2259.

Rohde R. and Price P. 2007. Diffusion-controlled metabolism for long-term survival of single isolated microorganisms trapped within ice crystals. *Proceedings of the National Academy of Sciences* 104:16592–16597.

Rudnick S., and Chen R. 1998. Laser-induced fluorescence of pyrene and other polycyclic aromatic hydrocarbons (PAH) in seawater. *Talanta* 47:907–919.

Rull F., and Sansano A., et al. 2010. ExoMars Raman laser spectrometer overview. *Proceedings of SPIE* 7819: 781915–781911.

Schuerger A., Fajardo-Cavazos P. et al. 2008. Slow degradation of ATP in simulated Martian environments suggests long residence times for the biosignature molecule on spacecraft surfaces on Mars. *Icarus* 194:86–100.

Sephton M. A. 2002. Organic compounds in carbonaceous meteorites. *Natural Product Reports* 19:292–311.

Shaw A. M., 2007. *Astrochemistry: From astronomy to astrobiology*. England: Wiley, pp

Sims M., Cullen D. et al. 2005. The specific molecular identification of life experiment (SMILE). *Planetary and Space Science* 53:781–791.

Sohn M., Himmelsbach D. et al. 2009. Fluorescence spectroscopy for rapid detection and classification of bacterial pathogens. *Applied Spectroscopy* 63:1251–1255.

Stalport F., Coll P. et al. 2009. Investigating the photostability of carboxylic acids exposed to mars surface ultraviolet radiation conditions. *Astrobiology* 9:543–549.

Storrie-Lombardi M. and Sattler B. 2009. Laser-induced fluorescence emission (L.I.F.E.): In situ nondestructive detection of microbial life in the ice covers of Antarctic lakes. *Astrobiology* 9:659–672.

Storrie-Lombardi M., Muller J. et al. 2008. Potential for non-destructive astrochemistry using the ExoMars PanCam. *Geophysical Research Letters* 35:L12201.

Storrie-Lombardi M., Muller J. P. et al. 2009. Laser-induced fluorescence emission (L.I.F.E.): Searching for Mars organics with a UV-enhanced PanCam. *Astrobiology* 9:953–964.

Vago J., Gardini B. et al. 2006. ExoMars: Searching for life on the red planet. *ESA Bulletin* 126:17–23.

Weinstein S., Pane D. et al. 2008. Application of pulsed-excitation fluorescence imager for daylight detection of sparse life in tests in the Atacama Desert. *Journal of Geophysical Research* 113:G01S90.

Yen A., Kim S. et al. 2000. Evidence that the reactivity of the Martian soil is due to superoxide ions. *Science* 289:1909–1912.

Ziegmann M., Abert M. et al. 2010. Use of fluorescence fingerprints for the estimation of bloom formation and toxin production of *Microcystis aeruginosa*. *Water Research* 44:195–204.

Zolotov M. and Shock E. 1999. Abiotic synthesis of polycyclic aromatic hydrocarbons on Mars. *Journal of Geophysical Research* 104:14033–14049.